Macromolecular Modification of EPDM: Wettability, Miscibility, and Morphology Study

MILENA GINIC-MARKOVIC,[1] NAMITA ROY CHOUDHURY,[1] MARIA DIMOPOULOS,[1] JANIS MATISONS,[1] CHANDIMA KUMUDINIE[2]

[1] Polymer Science Group, Ian Wark Research Institute, University of South Australia, The Levels, South Australia 5095, Australia

[2] Polymer Research Center, Department of Chemistry, University of Cincinnati, Cincinnati, Ohio 45221-0172

Received 2 May 2000; accepted 2 June 2000

ABSTRACT: The present investigation deals with studies on wettability, miscibility, and morphology of the macromolecularly modified EPDM. Two different maleated EPDM rubbers (grafted rubber) were chosen (0.5 and 1% maleation) for such modification and they were used in various proportions. Wettability of the rubber substrate, as observed from dynamic contact angle measurement, was improved using these grafted rubbers. Results of X-ray photoelectron spectroscopy showed an increase in oxygen level with higher levels of grafted rubber in the blends. Morphology study by transmission electron microscopy showed a smaller domain size for the blend with higher maleic anhydride content in the grafted rubber. The viscosity versus blend ratio results showed a negative deviation behavior for blends with 1% grafted rubber, whereas a positive negative deviation behavior was observed in blends with 0.5% grafted EPDM. As the strength of interaction increased, the glass transition shifted to a higher temperature. All blends were heterogeneous, as indicated by different degrees of dispersion. © 2001 John Wiley & Sons, Inc. J Appl Polym Sci 80: 2647–2661, 2001

Key words: blends; EPDM rubber; grafted rubber; miscibility; morphology; wettability

INTRODUCTION

Elastomeric compounds are selected for a particular application on the basis of their specific physical, electrical, or chemical properties. Not all the elastomers possess the required physical and chemical properties. For example, ethylene–propylene–diene rubber (EPDM) is selected for automotive window-seal application because it has very good ozone and weather resistance, although its hydrocarbon nature leads to relatively poor surface chemical properties and hydrophobicity, making it difficult to bond to polyurethane (PU) coating.

Because the hydrocarbon nature of EPDM rubber results in poor bondability, many attempts have been made by several workers to improve it. Vanderaar et al.[1] reported a new aqueous bonding system, to improve the adhesion of EPDM rubber to stainless steel. To improve wettability of the surface and biocompatibility of the ethylene–propylene rubber (EPR), grafting with 2-hydroxyethylene methacrylate (HEMA) and *N*-vinylpyrrolidone (NVP) was undertaken using CO_2-pulsed laser as an excitation source.[2] Later, Haddadiasi and Burford[3] extended previous studies by modification of four vulcanized EPR with

Correspondence to: N. Choudhury (E-mail: Namita.Choudhury@unisa.edu.au)

Journal of Applied Polymer Science, Vol. 80, 2647–2661 (2001)

acrylamide (AAM), HEMA, and NVP using a simultaneous radiation method. They monitored the effect of bulk modification on surface properties using contact angle. Limited plasma work carried out on EPDM shows improvement in adhesion to polyurethane, even when the time of exposure is low.[4]

In general there are two main ways of tailoring adhesion between the rubber and the coating. Either the coating should be designed for the nonpolar rubber surface, or the nonpolar EPDM should be designed to conform to the polar coating system. The present work deals with the latter approach. The wettability and adhesion of such hydrophobic polymer can be significantly improved either by surface modification or by macromolecular modification. In the present case, the EPDM rubber was macromolecularly modified. Bulk modification was achieved by blending EPDM with maleated EPDM.

Various factors of elastomer blends, for example, general behavior and miscibility, the thermodynamic factors, the processing parameters for their preparation, were previously reported by Roland.[5] The blends of EPDM rubber with different polymers were reported by several authors.[6,7] The effects of ethylene/propylene (E/P) content in the EPDM rubber, blending temperature, rotor speed, mixing time, and so forth, on the melt rheology of ethylene–propylene block copolymer and EPDM rubber blends have been studied by Maity and Xavier.[8] Go and Ha[9] reported that the addition of bis (3-triethoxysilyl propyl) tetrasulfide (TESPT) in EPDM/BR (butadiene rubber) blends increased the weight of bound rubbers and provided better dispersion of carbon black, resulting in good mechanical properties of vulcanized EPDM/BR blends. It was previously reported that maleic anhydride–modified EPDM improves the cure compatibility with natural rubber (NR). NR-EPDM blends containing 30–40% modified EPDM exhibit better mechanical properties and ozone resistance than those containing unmodified EPDM.[10] Yu[11] reported an application of maleated EPDM as a compatibilizer in magnetic rubber (EPDM-based) to be used in a magnetic sealing system. Maleated EPDM compatibilizer accelerates curing and also enhances compound physical properties.

Despite numerous studies on blends of EPDM rubber, very little has been reported on the bulk modification of EPDM to improve adhesion with a polar substrate, such as a PU coating. The current study deals with the blends of EPDM rubber with maleated EPDM (grafted rubber). Two different maleated rubbers were chosen because of their architectural similarity with EPDM rubber. The contact angle, X-ray photoelectron spectroscopy (XPS), and photoacoustic infrared spectroscopy (PA-FTIR) were used to investigate the wettability and the surface characteristics of the blends. In addition, to develop a useful polymer blend, it is important to know the rheological properties of the components and to understand the interaction and reactions between them. The apparent viscosity of the components in the blend and the effect of blend ratio on the apparent viscosity of the master batch at different shear rates were investigated using a Monsanto Processability Tester (MPT; Monsanto, St. Louis, MO). The effect of the viscosity ratio λ and the principal normal stress difference σ_E on the size and shape of the dispersed phase for grafted-EPDM/EPDM blends were examined in this study. The morphology of these blends was studied by transmission electron microscopy (TEM). The degree of dispersion and miscibility were investigated by dynamic mechanical analysis (DMA).

EXPERIMENTAL

Materials Used and Blend Preparation

The raw materials used and their characteristics are given in Table I. The compositions of the blends studied are given in Table II. The following blends were investigated: gum blends (pure rubber blends), black master-batch blends, and final batches with sulfur/accelerator. The gum blends were studied as model systems and the master-batch blends and final batches are representative of window-seal product formulations. Blending of pure components was done in an open two-roll mill and these were used as gum blends. The black master-batch compound was prepared using these gum blends and other ingredients. The formulation of the master batch is as follows: particular blend, 100 phr; carbon black (N660), 138 phr; ZnO, 5 phr; Aktiplast, 3 phr; hydrocarbon resin, 2 phr; polyethylene glycol, 1.5 phr; factice, 10 phr; stearic acid, 1 phr; PE wax, 3 phr; oil, 80 phr; and antioxidant, 0.5 phr. These master batches were designated with a suffix m and were mainly used for rheological studies. For studying the surface character of the final batch, a few final batches were prepared by adding sulfur (1.55 phr) and accelerators [Vulkacit DM

Table I Characteristics of the Raw Materials

	EPDM	Maleated EPDM	
Material	JSR EP103AF	Royaltuf 485	Royaltuf 490
Supplied by	Japan Synthetic Rubber (JSR)	Uniroyal USA	Uniroyal USA
Maleic anhydride	—	0.5%	1%
Ethylene content	63%	75%	55%
Iodine number	15	10	17
M_w [a]	6.6×10^5 Polydispersity 4.55	—[b]	5.9×10^5 Polydispersity 3.97
Crystallinity[c]	—	9.8%	—
T_g (°C)	−50	—	−47

[a] Determined by GPC under conditions described in Experimental section.
[b] Sample cannot be dissolved in THF under the experimental conditions. Polydispersity = M_w/M_n.
[c] DSC was carried out on the gum EPDM and EPDM-maleated rubber. Brazier and Nickel[42] reported that EPDM of ethylene content > 60% exhibits an endothermic transition at 47°C.

(dibenzthiazyl disulfide), 0.97 phr; MBT (2-mercaptobenzothiazole), 0.58 phr; TMTD (tetramethylthiuram disulfide), 0.66 phr; Butazate (zinc di-*n*-butyldithiocarbamate), 0.40 phr; ZDC (zinc diethyldithiocarbamate), 0.22 phr] in the second stage of mixing to the EPDM rubber compound and the master-batch blend compounds. These systems are designated with a suffix c (such as S_{1c}), where c indicates the presence of curatives.

The 2-mm-thick flat sheets were prepared from the gum blends by compression molding between two Mylar sheets (polyethylene terephthalate) at 100°C for 4 min under a pressure of 25 MPa. After the molding, the samples (still under compression) were immediately cooled by water to maintain the overall dimensional stability of the sheet. These sheets were stored at room temperature for 24 h and subsequently used for wettability, morphology, and dynamic mechanical studies.

Measurement of Wettability, Surface Characteristics, and Adhesion

Contact Angle of the Pure Components and the Blends

Static and dynamic contact angles for different rubber samples were determined using the sessile drop and Wilhelmy techniques at 25°C (relative humidity 65% in a clean room). The surface energies of the final batches were determined by the sessile drop technique[12,13] using water and glycerol (analytical grade). The statistical error in

Table II Blend Compositions

Component %	100/0	75/25	50/50	0/100
	Gum Rubbers and their Blends			
JSR EP 103AF pure EPDM	S_0	—	—	—
JSR/Royaltuf 485 (0.5% of maleic anhydride)	—	M_1	M_2	M_4
JSR/Royaltuf 490 (1% of maleic anhydride)	—	P_1	P_2	P_4
	Masterbatch Blends			
JSR EP 103AF	S_{1m}	—	—	—
JSR/Royaltuf 485	—	M_{1m}	M_{2m}	M_{4m}
JSR/Royaltuf 490	—	P_{1m}	P_{2m}	P_{4m}
	Final Blends			
JSR EP 103AF	S_{1c}	—	—	—
JSR/Royaltuf 485	—	M_{1c}	M_{2c}	M_{4c}
JSR/Royaltuf 490	—	P_{1c}	P_{2c}	P_{4c}

contact angle measurements was ±3% using five samples. The advancing and receding angles were determined for the pure polymers, their gum/master-batch blends, and the final blend compositions by the scanning Wilhelmy plate method[14] using water as the probe liquid. The technique essentially involves measuring the weight of the liquid meniscus attached to a solid when in contact with a probe liquid. The relation between the sensed force F and contact angle θ is as follows:

$$F = p\gamma \cos \theta + \rho_s v_s g - \rho_1 v_1 g \quad (1)$$

$$\theta = \cos^{-1}[F_{a,r}\ (d = 0)]/p\gamma \quad (2)$$

where p is the plate perimeter; γ is the liquid surface tension; ρ_s and ρ_l are the densities of the solid and the liquid, respectively; v_s and v_l are the total volume of solid and the volume of solid immersed in liquid, respectively. The relation proposed by Fowkes[15] has been used to calculate the surface energy $\gamma_s = \gamma_s^d + \gamma_s^p$, where γ_s^d and γ_s^p are calculated using the following equation:

$$1 + \cos \theta = 2(\gamma_s^d)^{1/2}(\gamma_1^d)^{1/2}/\gamma_{1v} + 2(\gamma_s^p)^{1/2}(\gamma_1^p)^{1/2}/\gamma_{1v} \quad (3)$$

The work of adhesion w_a was also calculated from the contact angle as follows:

$$w_a = \gamma_1(1 + \cos \theta) \quad (4)$$

where γ_l is the surface tension of the liquid, and θ is the contact angle.

X-ray Photoelectron Spectroscopy (XPS) Analysis

XPS experiments were carried out on the final batch samples (because these compounds are coated with polyurethane coating) using a Perkin–Elmer PHI 5100 XPS (Perkin–Elmer, Palo Alto, CA) using MgK_α X-ray source operating at 15 kV and 20 mA at an incident angle of 45° at a residual pressure of 1.33×10^{-7} Pa and at a pass energy of 93 eV. Surface compositions were calculated for each element using the respective sensitivity and the area of respective photoelectron peak from the spectra.

For all samples used for surface analysis, every care was taken to ensure that the surface was free of commonly encountered contaminants, by keeping them between Mylar sheets. No detergent or solvent wiping method was used because all samples studied were unvulcanized.

Photoacoustic Infrared Spectroscopy (PA-FTIR)

PA-FTIR was done on pure elastomers and their blends using a Nicolet Magna Spectrometer (Model 750; Nicolet Instruments, Madison, WI) equipped with an MTEC (Model 300) photoacoustic cell. The sample was placed in a circular stainless steel cup (3 mm deep, 10 mm diameter) and sealed in a device with a potassium bromide salt window, and a helium atmosphere to promote good heat transfer. Carbon black was used as a reference because it absorbs all wavelengths of the infrared radiation and produces a spectrum that mirrors both the energy characteristics of the detector and the optical performance of the instrument. The resolution of 8 cm^{-1}, 256 scans, and mirror velocity of 0.158 cm s^{-1} were used.

Gel Permeation Chromatography (GPC)

Determination of molecular weight was carried out using a Waters 2690 GPC unit equipped with a Waters 410 refractive index detector (Waters Instruments, Rochester, MN). Tetrahydrofuran (THF) was used as an eluting solvent. A calibration curve for a linear THF column was first prepared using polydimethyl siloxane (PDMS) molecular weight standards. Thus all results obtained from the GPC were molecular weights relative to PDMS. A linear mixed-bed ultrastyragel Waters column was used (dimensions of 7.8 × 30 mm) for the measurement of molecular weight in the range 2,000–4,000,000.

Preparation of Samples for Adhesion and Measurement of Strength of Adhesion

To prepare adhesion samples thin sheets of pure EPDM and grafted rubbers were made first with fabric backing, by molding technique, under a pressure of 25 MPa at 100°C. Two sheets were then brought in contact with each other under light pressure (a few kPa) at room temperature and kept for 24 h. The 180°-peel test was performed on 20-mm-wide samples for measuring the adhesion strength. All the adhesion measurements were carried out using a Monsanto Tensiometer at room temperature and at crosshead speed of 50 mm min^{-1}. The adhesion strength reported is an average adhesion strength of five samples, and was calculated using the following formula:

$$G_a = 2F/w \quad (5)$$

where G_a is the adhesive strength, F is the peeling force, and w is the width of the sample.

Scanning Electron Microscopy (SEM)

Because the appearance of the surface generally changes during a peel test, microscopic information is very useful in determining the mechanism of adhesive failure. All the surfaces after adhesion failure were examined by SEM, using a Cam Scan CS44 operating at an acceleration voltage of 20 kV.

Miscibility and Morphology Study

Rheological Study

The effectiveness of blending was examined by studying the morphology and miscibility by various techniques. The viscosity of the components and the variation in blend viscosity with grafted rubber concentration at a particular shear rate were studied by using a Monsanto Processability Tester (MPT) 83077. This is a constant-volume capillary rheometer in which the viscosity of the rubber and rubberlike thermoplastic elastomers can be determined in two different ways:

1. Direct way for measuring viscosity (under viscous mode)
2. Indirect way under stress mode

MPT was used in the stress mode with varying test temperatures (80–100°C) and shear rates (122.6–1226 s^{-1}). The experiments were carried out using a capillary die of $L/D = 30$, where D is the capillary diameter (1 mm) and L is the length of the capillary (30 mm). In analyzing data from the MPT test, no corrections were made because of the large L/D ratio of the capillary die: multiple die entry angles of 45 and 60° minimize the pressure drop and no correction is needed. After leaving the MPT capillary, the extrudate passed a scanning laser device, which measured its diameter as a percentage of the capillary diameter. Running die extrudate was measured as the extrudate passed the scanning laser device during steady flow. The principal normal stress difference σ_E was calculated from the die swell using the following equation[16]:

$$\sigma_E = \frac{(2 + \gamma_m)\gamma_m}{2(1 + \gamma_m)} (2\tau_{12}) \quad (6)$$

where τ_{12} is the shear stress and γ_m is the maximum recoverable deformation.

Transmission Electron Microscopy (TEM)

The most straightforward method of examining the structure of the multiphase polymeric systems is direct observation of the morphology by TEM. With a very high resolution limit as low as a few angstroms, the electron microscope can be used to probe the elastomer blends for the degree of dispersion. A piece of each sample approximately 1 × 1 × 5 mm was mounted on an appropriate specimen holder, which was then placed into a cryostatic chamber of an ultramicrotome (FC 4D, Reichert-Jung Co.) The entire slicing area was maintained below the glass-transition temperature (T_g) of the sample. Because of the natural contrast of grafted rubber and EPDM, staining was not done. Specimen slices, having a thickness of about 90 nm, were produced using a diamond knife and were collected on carbon-coated grids. These specimens were examined in transmission using a JEOL 100CX II electron microscope (JEOL, Peabody, MA) operating at 80 kV.

Dynamic Mechanical Analysis (DMA)

DMA was carried out on the gum rubber samples (pure components and the gum blends) using a DMA 2980 (TA Instruments, USA) operating in tension mode from −100 to 100°C at 1-Hz frequency and 0.2% strain amplitude, at the programmed heating rate of 2°C min^{-1}. Liquid nitrogen was used to achieve subambient conditions. The T_g of the blends was determined from the tan δ and loss modulus curves. The effect of composition on T_g value was calculated using the Fox relationship[17] and correlated with the observed T_g as follows:

$$\frac{1}{T_{g,b}} = \frac{w_1}{T_{g,1}} + \frac{w_2}{T_{g,2}} \quad (7)$$

where w_1 and w_2 represent the weight fractions of the respective components and $T_{g,b}$, $T_{g,1}$, and $T_{g,2}$ are T_g's of the respective blend, component 1, and component 2.

RESULTS AND DISCUSSION

Wettability, Adhesion Strength, and XPS Studies

To investigate the mutual affinity of the component elastomers, which is necessary for good per-

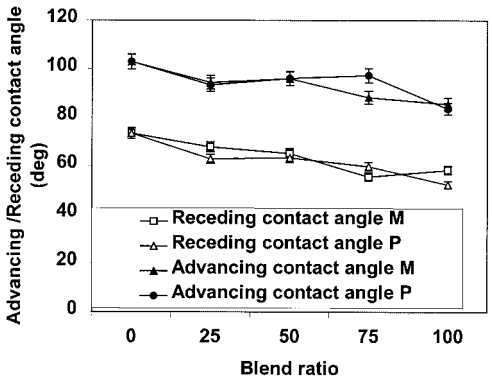

Figure 1 Advancing and receding contact angles of gum rubber blends: EPDM/0.5% maleated EPDM (M) and EPDM/1% maleated EPDM (P).

formance, dynamic wettability was measured on the pure polymers and their blends using water as the probe liquid. Table II summarizes the blend composition. Pure EPDM rubber is designated as S_0, and pure 0.5% maleated EPDM and its blends are designated by M series and 1% maleated EPDM and its blends as P series. The maleated rubbers were used in both 25 and 50 wt % levels to EPDM. Figure 1 shows the effect of blend ratio on the advancing and receding contact angles of pure components and the gum rubber blends. The contact angle in water decreases for both 25 and 50 wt % compositions of blends of both maleated EPDMs (0.5 and 1% maleation); however, the rate of decline is more or less similar in both cases. The receding contact angle also shows a similar trend. It must be noted that the receding contact angle is much lower than the advancing one. The contact angle measurement indicates that the surface probed by the advancing angle is much more hydrophobic than the one probed by the receding angle, hence a dynamic behavior of the sample surface is evident, which is environment dependent. In some cases, swelling by solvent or water permeation can cause such time-dependent hysteresis. To avoid all those effects, all our measurements were carried out for a short time and at a higher-stage velocity. A decrease in both advancing and receding contact angles indicates that both P and M series blends improve their hydrophilicity for different compositions. This may be ascribed to the improved chain mobility and polarity on the surface from the bulk. Generally, blending leads to conformational changes and surface restructuring attributed to improved chain mobility, and accumulation and orientation of polar sites on the surface from bulk, as a result of physical interaction. It is clear from the graph that the level of interaction varies with the type of grafted rubber and the blend ratio. At a certain blend ratio, the change in surface structure exhibits an optimum hydrophilicity and wettability. As the blend of 75% of grafted rubber does not show marked improvement in contact angle, it was not taken into consideration for final blend preparation.

The wettability characteristics are sensitive not only to the geometry of the surface heterogeneities but also to the wetting liquid. Extrand and Kumagai[18] reported the increase of the contact angle of four different wetting liquids studied with increasing their surface tension. The wetting cycle measurement carried out with chosen gum rubber blends in water also gives insight into the roughness and mobility of the surface structure besides the contact angle measurement.[19] It was found that the advancing and receding contact angles, calculated from the Wilhelmy technique for gum blends, are different and show considerable hysteresis resulting from the surface heterogeneity. A wetting cycle of the gum blends in water is shown in Figure 2. It consists consecutively of forced and spontaneous movements. Section A–C corresponds to forced advancing water movement at constant velocity (100 μm s^{-1}) and section B–C corresponds to the advancing buoyancy slope, where the contact angle remains essentially constant. At C, the forced motion is stopped and spontaneous relaxation of the three-

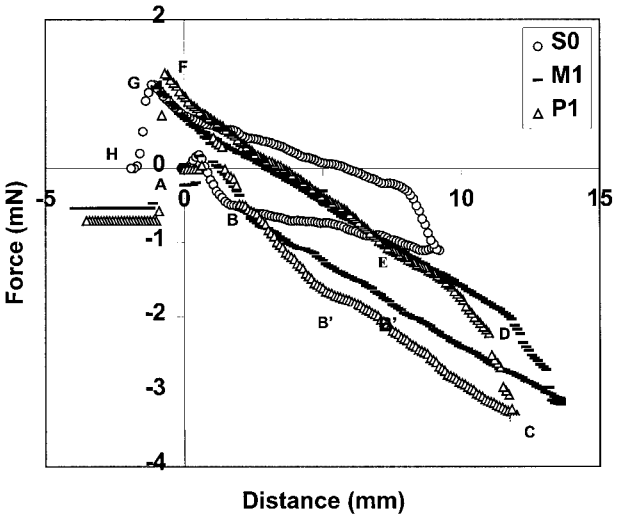

Figure 2 Wetting cycle of the gum EPDM rubber (S_0) and its blends with 25% of 0.5% maleated EPDM (M_1) and 25% of 1% maleated EPDM (P_1) in water.

phase contact line (TPCL) occurs. The contact angle then decreases. Over D–H, forced receding water movement ($V = 100\ \mu m\ s^{-1}$) takes place. Section E–F corresponds to the receding buoyancy slope (similar to the advancing counterpart). At F, forced motion is stopped. Further forced receding movement of liquid (G–H) results in eventual breakage of solid–liquid contact. In this system (Fig. 2), at the substrate–water interface, the water phase did not wet the substrate, and the contact angle is greater than 90° with the force decreasing. All samples were immersed up to 10 or 14 mm. The hysteresis could be related to the flexibility of the elastomer chains and could be ascribed to the different degrees of freedom of the polymer backbone in each case. The backbone allows the exposure of the pendant group to the maximum effect, such that they are away from the surface when in air, but towards the surface in water, a case that is similar to that in siloxane backbone polymer.[20,21]

Polymeric surfaces can restructure in response to a change of the interfacing phase, to tune their surface properties with the properties of the interfacing medium, such as poly(2-hydroxyethylmethacrylate) (PHEMA), exposing hydrophobic methyl groups at the polymer–air interphase but hydrophilic hydroxyl groups at the polymer–water interphase.[22] As a result, this gives a relatively low receding contact angle and high advancing angle. In general macromolecules on surfaces have a greater freedom than do their bulk counterparts, and appear as zones of enhanced mobility resulting from the decreased surface density and, hence, free volume.[23] The macromolecular dynamics, which deeply affect the bulk properties of polymers, must also be taken into account in the description of surface properties. However, because of much greater mobility of the chains of polymer surfaces than of those from the bulk, the use of the bulk values such as glass-transition temperature to gauge both the occurrence and the extent of surface dynamic phenomena can be misleading.[24] In general the water contact angle hysteresis is found to be less in M_1 than in S_0 and P_1. This may be the result of a loss of rotational freedom in that blend with high ethylene content and 0.5% maleic anhydride in grafted EPDM. Moreover, the molecular weight distribution, as shown by GPC for P_4 or S_0, is fairly wide, so there may be a tendency of the low molecular weight end to orient toward the surface in those cases. The blends in each case have a lower contact angle value than that of the control

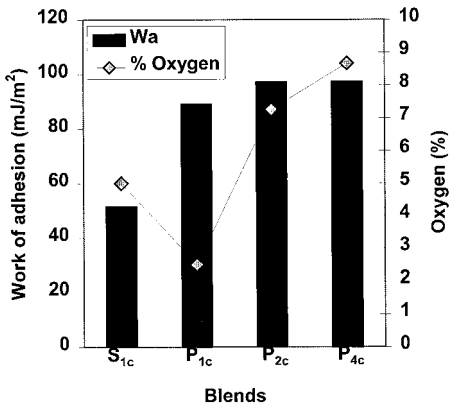

Figure 3 Co-relation between the level of oxygen and work of adhesion of final blends with different proportions of 1% maleated EPDM.

EPDM rubber. Concomitantly, the work of adhesion [calculated from eq. (4)] of the final batches, which is the work done to separate the solid and the liquid, increases (Fig. 3). The work of adhesion is at a maximum for grafted rubber samples with water as the probe liquid.

For quantitative estimation of chemical elements on the surface, XPS studies were undertaken. Survey spectra of samples M_{4c} and P_{4c} are shown in Figure 4. The spectra exhibit two major peaks at about 534 and 284.5 eV, corresponding to O_{1s} and C_{1s} photoemission. The respective position of each element does not change, although the quantity changes. Atomic composition obtained from multiplexed spectra of the oxygen photoemission is mainly calculated to assess the hydrophilicity. Figure 5 shows the representative plot of the C_{1s} peak of sample M_1 in the range of 282–292 eV. It is clear from the C_{1s} peak that it exhibits a broad tail, which corresponds after charge correction to 284.5, 286, and 288 eV and is related to C—H, C—O, and C═O bonds, respectively. The intensities of these peaks vary with different blends. The level of oxygen is reported on the final batch samples of the various rubber compounds (because this compound is finally coated). To correlate the surface behavior with thermodynamic work of adhesion, the contact angle was also measured on these samples.

Figure 3 shows the effects of blending grafted rubber with EPDM on the level of oxygen and work of adhesion. As the proportion of the grafted rubber increases in the final uncured blends, the contact angle decreases, which indicates the polar nature of the surface. In particular, the sample P_{2c} shows a lower value of the contact angle and

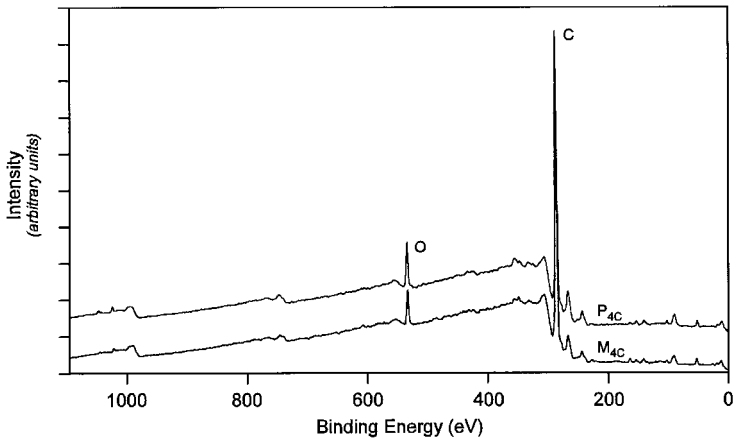

Figure 4 XPS trace of compounds of 100% maleated EPDM with 0.5% maleic anhydride (M_{4c}) and 1% maleic anhydride (P_{4c}).

hence higher wettability of the surface resulting from a higher maleic anhydride (1%) content. Therefore, the lower the angle, the higher the surface polarity, so the better the work of adhesion as determined using eq. (4) and shown in Figure 3. At the same time, an increased polarity is observed in both cases, except for P_{1c}, with increasing levels of oxygen and blend ratio. This sample shows a very low level of oxygen content. Such low surface oxygen content in this case could only be the result of surface reorganization. Generally, surface reorganization can occur by two different methods, either (1) by diffusion of low molecular weight materials into/from the bulk or (2) by macromolecular motion, allowing the polar group to reorient away from the surface.

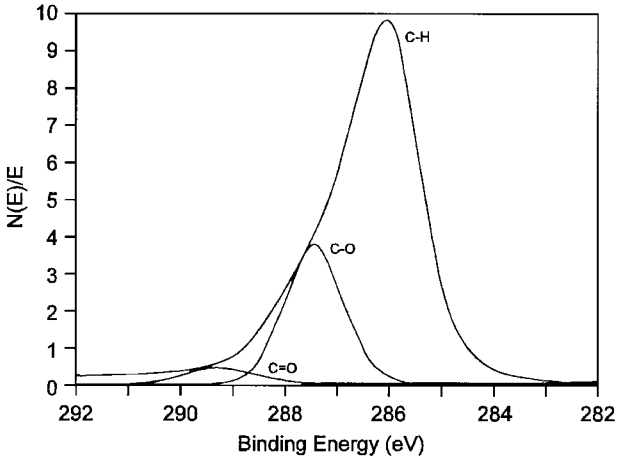

Figure 5 Carbon (C_{1s}) envelope of gum rubber blend with 25% maleated EPDM with 0.5% maleation (M_1).

Based on the discussion on diffusion/migration of additives in our earlier study,[25] we know that appreciable diffusion of low molecular weight additives occurs only after 7 days. In this case all samples were stored in a controlled environment and experiments were performed within that time. Therefore, molecular rearrangement, which occurred to the outermost atomic layer of P_{1c} within this time, is responsible for and noticed as decreased surface oxygen. Oxygen levels present in the P_{4c} and M_{4c} samples can also be detected in Figure 4. An oxygen peak is obvious in both samples, indicating a slightly higher concentration of oxygen in P_{4c} (8.67%) than that in M_{4c} (6.69%). Higher maleic anhydride content in P_{4c} (1%) indicates higher oxygen level on the surface and higher polarity.

Although the increased polarity is not observed in P_{1c} from XPS (oxygen level), the calculated polar component of surface energy exhibits the highest value in P_{1c} (Fig. 6). In addition, it is interesting to note that XPS sampling depth is about 10 nm compared to that of the very thin layer of the surface probed by the contact angle. The difference in depth profiling encountered by those two techniques, together with the macromolecular reorganization, diffusion of low molecular weight additives, and restructuring of the polymer surface with regard to the interfacing medium, caused the difference in polarity of P_{1c} tested by the above-mentioned techniques. It must be mentioned here that unvulcanized EPDM rubber compound and blend surfaces have physical and chemical heterogeneity,[25] exhibiting metastable contact angles. The surface energy of

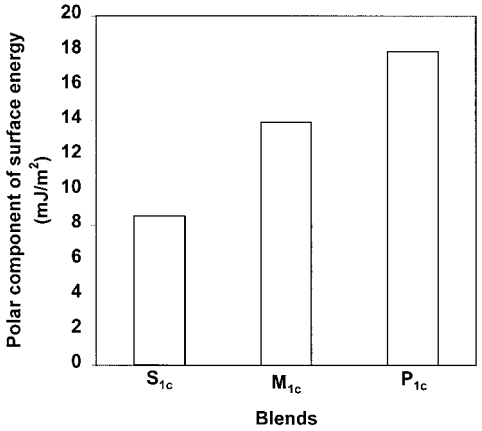

Figure 6 Effect of bulk modification on the surface energy of final blends with 25% maleated EPDM with 0.5% maleic anhydride (M_{1c}) and 25% maleated EPDM with 1% maleic anhydride (P_{1c}) relative to control sample (S_{1c})

various samples (e.g., S_{1c}, M_{1c}, and P_{1c}) was determined by the sessile drop technique and the effect of maleic anhydride content on the polar component of surface energy was investigated using both water and glycerol. The total surface energy of the blends does not change very much (16–20 mJ m^{-2}). However, the respective polar component represented on the plot increases with the maleic anhydride level in the modified EPDM rubber. The polar component of surface energy is the highest in P_{1c}, confirming the higher polarity of the blend with higher maleation (1% maleic anhydride). Moreover, the fractional polarity x_p (given by γ_s^p/γ_s) increases with maleic anhydride level, from 0.412 for S_{1c} to 0.949 for P_{4c}. Several authors reported behavior of acrylic grafted polyolefin surfaces with respect to the interfacing medium.[26,27] In the air the surface displays apolar characteristics but in the polar interfacing environment acrylic grafts become exposed.

The mutual affinity between two components can also be clearly demonstrated by measuring adhesion strength. The adhesion strength between the pure components was measured by the 180°-peel test on 20-mm-wide specimens using eq. (5), whereas S_0/M_4 joints display an adhesion strength of 275 J m^{-2} (interfacial) the S_0/P_4 joints show a strength of 730 J m^{-2} (mixed failure). This is related to better adhesion of 1% grafted rubber to pure EPDM because of partial structural similarity [ethylene/propylene (E/P) ratio and better physical interaction]. Additionally, factors such as interdiffusion, green strength, and chain entanglement of the individual phase have significant roles in determining the strength of the joint and it is the interplay between these factors that decides the adhesion. It is important to note that E/P ratios of S_0 and P_4 closely match, which indicates better interdiffusion between these two phases, leading to the better adhesion. The surface of the sample after adhesion failure was examined under SEM and is shown in Figure 7 for the EPDM surface of peeled S_0/P_4. A large proportion of EPDM was observed to be taken by the surface of P_4. The surface is rough, the extent of which varies depending on the severity of the fracture. It shows cavities and fibrils all over the surface. The size of the cavities and their distribution on the surface corresponds to the EPDM taken out by the other surface (P_4), suggesting that the failure is mostly cohesive in nature within the EPDM phase. Both peeled surfaces were investigated. The intermolecular diffusion between the two phases, as measured by the peel test, can also be examined from the tensile fracture surface of the gum blends. The fracture surface of the blend, formed from the tensile experiment carried out at room temperature and a 500 mm min^{-1} rate, was examined by SEM and a representative micrograph for the system M_2 is shown in Figure 8, from which cavities and globules are noticed. They correspond to the dispersed phase and gel in the grafted rubber. Their extents vary with the blend composition. The disperse phase forms an adhesive bond during mixing by wetting and interdiffusion. Additionally, as mentioned earlier, interdiffusion is better in the S_0/P_4 joint because of partial similarity in its E/P ratio to that of the control rubber.

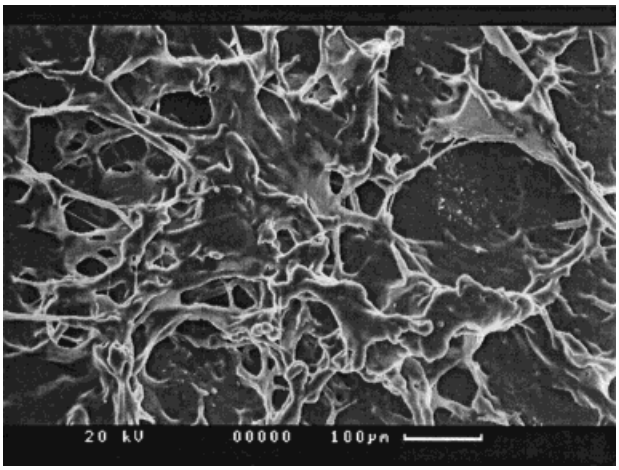

Figure 7 SEM photograph of peeled EPDM surface: EPDM side of S_0/P_4.

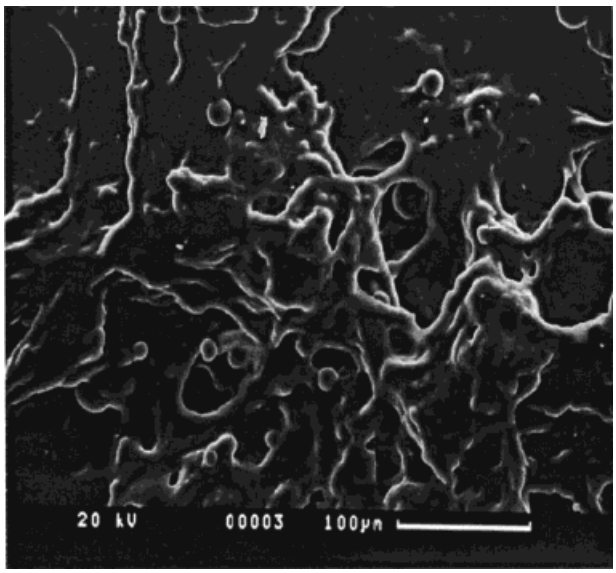

Figure 8 Tensile fracture surface of the gum rubber blend M_2.

PA-FTIR Spectroscopy

Depending on the mirror velocity chosen, PA-FTIR provides information about the molecular vibration of functional groups present on the surface layer for a few micrometers to those originating from the bulk. The pure polymers and their blends were examined for their surface characteristics by PA-FTIR at a slow mirror velocity. Figure 9 is a representative FTIR plot in the region of 600–1800 cm^{-1} for M_1 and M_2. Table III shows the characteristic peaks of blends and control sample obtained from the IR spectra. From the table, the change in wavelength of the bonds attributed to CO stretching and CO bending with the blend concentration is observed. The peak at 722 cm^{-1} is assigned to units of five or more methylene groups (in-phase rocking vibration) and is found to decrease on the surface of the blends as a result of the decrease of long ethylene sequences on the surface.

All the blends show absorption bands characteristic of acid anhydride, in the region of 1744 cm^{-1}. Generally, their positions depend on the ring size of the anhydride and also on the type of unsaturation. For cyclic anhydrides such as maleic anhydride, the C—O stretching appears in the region of 1300–1200 cm^{-1}, as a shoulder to the strong $–CH_2$ band at 1377 cm^{-1}. The peak at about 1461 cm^{-1} for the P blends results from the overlapping vibrations of methylene ($–CH_2–$) bending and methyl ($–CH_3$) asymmetric bending bands. On S_0 (pure JSR), it occurs at 1467 cm^{-1} and in M_4 and P_4 at 1461 cm^{-1}. Blends of 0.5% grafted rubber show intermediate bands resulting from these overlapping vibrations. Table III also shows the peak heights of 1744 and 722 cm^{-1} for different blends. The relative height remains almost constant or increases marginally with the maleated rubber in the blend. The height of the CH_2 band at 722 cm^{-1} increases with the ethylene content of the component polymer (S_0 ca. P_4 ca. M_4). Thus, for the M blends, it is quite comparable to the control, whereas the P systems show very low intensity of those peaks. This also indicates that macromolecular modification of the blends is sufficient to induce a change in the mobility of the polymeric chains and architecture on the subsurface. The preferential existence of the grafted compounds on the subsurface in some cases could well be related to their microheterogeneous structure, which is often the characteristic of grafted material. Such microheterogeneities are the result of the defects and microcavities and may be of various other forms.[28]

Miscibility and Morphology

Rheological Study and TEM

Besides thermodynamic factors, such as work of adhesion and interfacial tension, the miscibility and the morphology of the blends are also controlled by kinetic factors such as melt viscosity. Figure 10 shows the variation in viscosity with shear rate for raw materials. It is evident from the figure that the viscosity of P_4 is higher than that of M_4 and S_0. Generally, the higher E/P val-

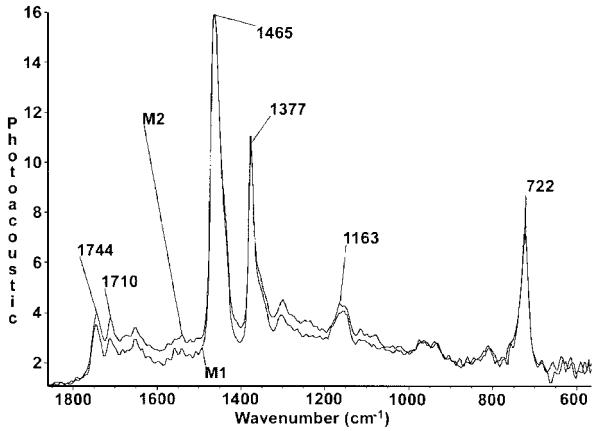

Figure 9 PA-FTIR spectra of gum rubber blends with 25% of 0.5% maleated EPDM (M_1) and 50% of 0.5% maleated EPDM (M_2).

Table III PA-FTIR Peak Assignment in the Region of 600–2000 cm^{-1}

Sample	$>CH_2$ Deformation	$—CH_3$ Group Stretching	Height of $>CH_2$ Band at 722 cm^{-1}	Height of >CO at 1744 cm^{-1}
S_0	1467	1380	23	—
M_1	1465	1377	23.2	3.5
M_2	1465	1377	20.3	3.0
M_4	1461	1376	34	3.7
P_1	1461	1378	2.1	0.4
P_2	1461	1377	3.3	0.8
P_4	1461	1378	12.1	3.4

ues in EPDM result in higher viscosity. Maity and Xavier[8] and Ghosh and Das[29] also reported a similar trend. However, in the present case the trend is opposite. P_4 (1% grafted rubber) reveals higher viscosity resulting from higher maleic anhydride content, regardless of the lower level of E/P, than that in M_4. Normally, grafting increases viscosity. Kubota[30] noticed that the presence of grafted polybutadiene in SAN increases the melt viscosity of ABS by 40–60% over that of pure SAN copolymer.

To predict the miscibility of the studied blends, the logarithmic rule of mixtures is applied at constant temperature and shear rate as follows[31]:

$$\log \eta = \phi_1 \log \eta_1 + \phi_2 \log \eta_2 \quad (8)$$

where η_1 and η_2 are the pure component viscosities at the same temperature, and ϕ_1 and ϕ_2 are their volume fractions.

Figure 11 shows the viscosity of different master-batch blends obtained from MPT. From this figure, it is obvious that the blends with different proportions of 1% maleated EPDM in EPDM show negative deviation behavior (NDB) at 122 s^{-1} shear rate and 100°C, thus indicating immiscibility. Generally, emulsion and suspension flows, which are used as models for immiscible blends, both suggest that the viscosity must increase with the volume fraction of the dispersed phase. The model proposed by Lin[32] corresponds to negative deviation from the log-additivity rule. This type of flow frequently has been observed in immiscible polymer blends. However, the positive negative deviation behavior (PNDB) is observed in the blends of M series. M_{1m} reveals partial miscibility, whereas the other blends with increasing level of grafted rubber show immiscibility. The PNDB phenomenon is primarily related to concentration-dependent interaction and can be explained in two possible ways: (1) partial miscibility at low concentration and (2) a concentration-dependent change of the flow mechanism in the immiscible region. The classification of the blends on the basis of the log-additivity rule and deviation from it relies on the flow mechanism, but not on the chemical nature, of the blends. Utracki and Fisa[33] reported on the blends of PET/PA-6,6 or PET/PA-6, which showed NDB behavior

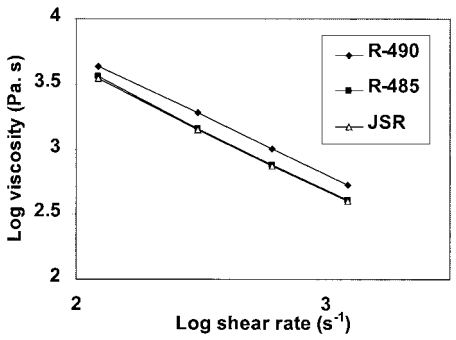

Figure 10 Viscosity of the gum rubbers.

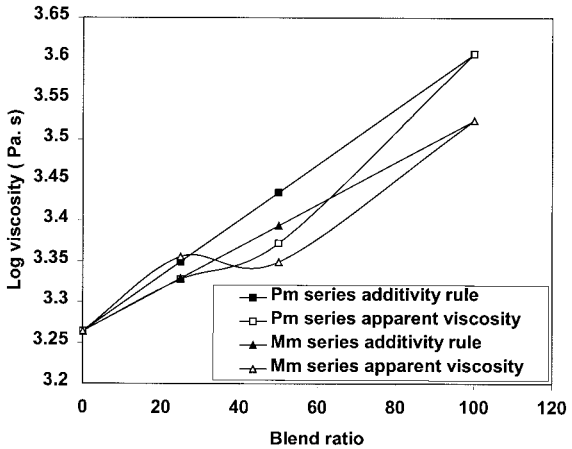

Figure 11 Effect of blend ratio on the viscosity of master batches with 0.5% maleated EPDM (M_m) and 1% maleated EPDM (P_m) at a shear rate of 122 s^{-1}.

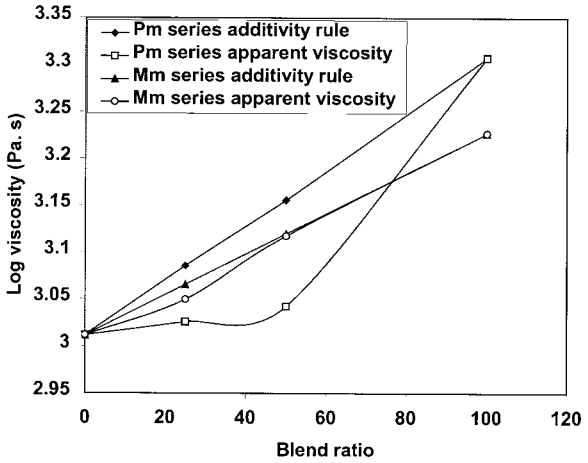

Figure 12 Effect of blend ratio on the viscosity of master batches with 0.5% maleated EPDM (M_m) and 1% maleated EPDM (P_m) at a shear rate of 306.5 s^{-1}.

with regard to viscosity and composition relationship. However, the depth of the negative deviation from the log-additivity rule remained invariant with the shear stress. Figure 12 shows the effect of blend ratio on the viscosity at a shear rate of 306.5 s^{-1}. It is interesting to note that the blends of both M and P series show NDB behavior but with increasing degree of negative deviation with shear rate.

In extrusion, the flow through the extruder dies is normally controlled by the steady shear behavior of the material. Therefore, besides the viscosity η, the viscosity ratio $\lambda = \eta_1/\eta_2$ (where η_1 indicates the viscosity of the dispersed phase and η_2 that of the matrix) and the first normal stress difference σ_E characterizes the flow behavior.

Table IV shows the viscosity ratio of the dispersed phase of grafted rubber (λ_M or λ_P) in the matrix S_0, at different shear rates. Between the two, λ_M shows a decrease with shear rate. However, λ_P initially increases up to a shear rate of 306.5 s^{-1} and then levels off. The difference in λ also results in variation of the extrudate morphology (e.g., different drop deformation, different shear segregation), which in turn changes the rheological response of the system. The resulting morphology thus depends, among other factors, on the relative magnitude of the first normal stress difference (σ_E) of the matrix and the dispersed phase. When σ_E of the dispersed phase is greater than that of the matrix, droplets are formed. Table V shows the first normal stress difference calculated from the die swell for EPDM and grafted EPDMs (σ_E S_0, σ_E M_4, σ_E P_4), at different shear rates. From Table V, it is clear that, at any shear rate, the first normal stress difference is higher for both the maleated EPDM rubbers than for that of EPDM, indicating droplet formation.

Table IV Viscosity Ratio at Different Shear Rates

Shear Rates (s^{-1})	λ_M	λ_P
122.6	1.03	1.23
306.5	1.01	1.35
613	1.01	1.34
1226	1.00	1.33

Table V First Normal Stress Difference of the Pure Components at Different Shear Rates

Shear Rates (s^{-1})	σ_E of P_4 (Pa)	σ_E of M_4 (Pa)	σ_E of S_0 (Pa)
122.6	943,596.1	836,052.9	768,046.4
306.5	951,103.5	766,163.3	713,810.9
613	956,165	871,694.8	680,108.6
1226	945,395.2	881,768.8	744,128.3

Generally, the morphology of a blend depends on two factors: (1) dispersion degree of the two phases and (2) the shape and dimensions of the dispersed particles. In turn, these factors are determined by the rheological characteristics of the two components and by the mixing conditions. Therefore, during mixing, it is important that the size of the dispersed phase is optimized because all the properties of a blend strongly depend on its state of miscibility. Corish[34] reported that with few exceptions, the elastomer blends are mostly microheterogeneous and the continuous phase in these materials is invariably found to be the rubber of low viscosity, provided it is present at a sufficiently high concentration.[35] In the present case the matrix is considered to be EPDM rubber because of its higher proportion, and the maleated rubber is the dispersed phase. The domains in such a heterogeneous blend can be directly observed under the electron microscope, provided that the electron density differences are of sufficient magnitude to provide contrast and extend over a difference greater than that of the instrument's resolution. In the present case, the morphology of the blends was studied by TEM. Figure 13 reveals the transmission electron micrograph of P_1. The domain size in the case of P_1 is found to

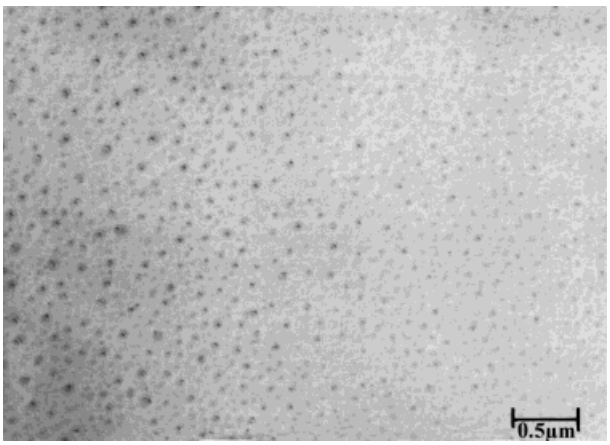

Figure 13 TEM photograph of the gum rubber blend with 25% of 1% maleated EPDM (P_1).

be 0.04 μm, which is smaller than that of M_1 (0.14 μm) and indicates better compatibility of the blend with a higher level of maleic anhydride in the grafted rubber. A similar trend was observed by Wu,[36] who reported that, during extrusion, the decrease in the dimensions of the minor phase of a chemically modified rubber system was significant, compared to the unmodified one, and related that to the low interfacial tension. In the present study, the smaller size of the dispersed component P_1 (0.04 μm), resulting from the chemically modified EPDM rubber with a higher level of maleic anhydride (1%), could well be attributed to the lowering of interfacial tension.

DMA Study

A popular method of deducing the degree of homogeneity in a polymer blend is from the measurement of the transition temperatures from rubbery to glassy behavior, by dynamic mechanical measurement. In addition, DMA is also a useful tool for approximate estimation of domain size in a two-phase blend and can resolve the effect of relatively minor changes in formulation or processing.

The glass-transition temperatures, obtained from DMA using the tan δ curve, are shown in Figures 14 and 15. In the M blends, the height of the transition decreases and width increases. Thus M_1 can be considered as partially miscible because of the appearance of a very broad transition. In the case of M_2 the breadth increases with the disappearance of the shoulder resulting from better phase interactions. The P blends show much sharper single peaks. The appearance of a single transition, however, cannot be taken as

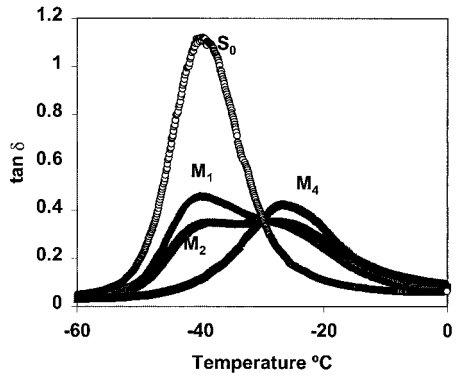

Figure 14 T_g's of gum rubbers and their blends with 0.5% maleated EPDM (M).

unambiguous evidence of miscibility of samples P_2 and P_1 (Fig. 15). A two-phase blend can exhibit a single intermediate glass transition when the domain size is small. Kaplan[37] reported that:

- Two T_g's are apparent in blends where the domain size is >0.1 μm.
- Two transitions will appear, but are broadened for domain size 0.02–0.1 μm.
- When domain size is <0.015 μm, the blend exhibits one glass transition.

Figure 14 shows that the M blends exhibit a broader transition compared to that of the pure components. Roland[38] also observed similar trend for blends of *cis*-1,4-polyisoprene and atactic poly(vinylethylene). Pure EPDM shows a T_g of -38°C, whereas the T_g's of M_4 and P_4 are -26 and -35°C, respectively. Blends of M series show T_g's intermediate between two parent polymers. However, the blends of the P series show only one T_g value. Normally, the T_g of a two-phase blend can

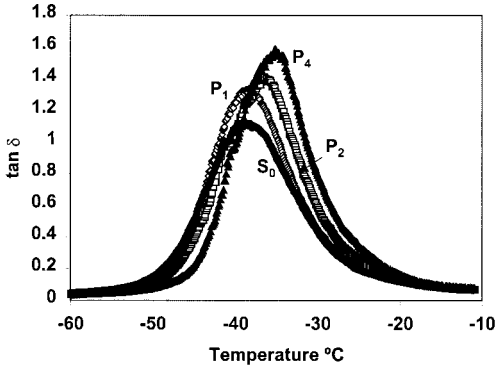

Figure 15 T_g's of the gum rubbers and their blends with 1% maleated EPDM (P).

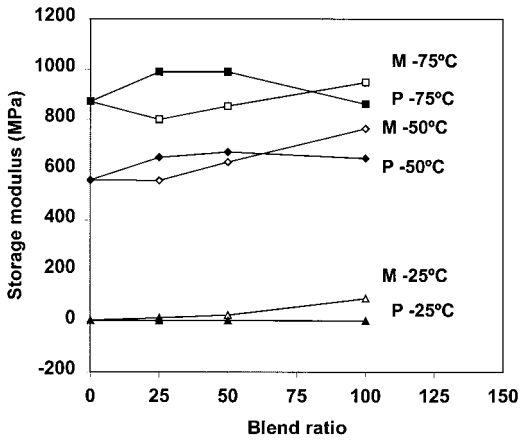

Figure 16 Storage moduli of all gum rubber blends studied.

be well characterized by two distinct peaks on the damping curve, provided the T_g's of the component polymers are well separated. In the P series, the T_g's of EPDM and P_4 are relatively close and the difference is only 3°C. In addition, P_4 shows low T_g compared to that of M_4. The difference in T_g's is mainly attributed to the free rotation of the polymer chains in the two compositions. The higher maleic anhydride content in P_4 allows the chain to rotate as a result of increased free volume, eventually lowering the T_g.

The effect of blend ratio on the storage moduli of different systems is shown in Figure 16. At any temperature the grafted rubber M_4 shows higher moduli than does the control because of higher ethylene content of this system. The E' of the blend compositions lies intermediate between the two controls. Interestingly, P_4 and S_0 show low E' at lower temperature, whereas the blends P_1 and P_2 show higher E' compared to that of the parent polymers. The increase in E' at subambient temperatures could well be attributed to better interaction between the two phases. The TEM micrograph also reveals very fine droplets of maleated rubber in P_1. It must be noted that the ethylene content is different in two grafted rubbers. M_4 has a higher ethylene content but a lower level of maleation.

DMA can be also used to characterize the morphology and interaction between the two components in a blend or composite. As the strength of interaction increases, the T_g moves to a higher temperature and the tan δ peak height decreases. A comparison of the damping peaks for two different maleated systems reveals a difference in the peak intensity (height). In a filled system, polyblend or grafted system, the intensity of the damping peak gives a qualitative estimate of the phase continuity and concentration. The greater the concentration, the larger the damping peak and the more likely it is that the phase is continuous; moreover, they give us information on miscibility. The extent of solubility and the size of the dispersed particles also influence the damping peak to some extent.[39] Figure 17 shows the effect of the blend composition on the glass-transition temperature obtained from loss modulus. From the figure a negative deviation of the T_g's of different blend compositions is observed with respect to the imaginary straight line obtained using eq. (7) (shown as unfilled points on the plot). However, for the P series that deviation is marginal. The depth of the deviation is more pronounced in the case of the M series. Although a single T_g is observed, it is less in all cases than the predicted value [obtained using eq. (7)]. This could be the result of local orientation effects promoted by interaction between two different types of EPDMs.[40]

In general, all the blends are heterogeneous. Although a single T_g is observed, in general that is a measure of the degree of dispersion, not of miscibility. Because the rheological measurements were carried at $T > T_g$, and if the polymers were miscible at T_g, it does not necessarily indicate that thermodynamic miscibility exists under the rheological test conditions.[41]

CONCLUSIONS

- The wettability of an EPDM compound, as observed from dynamic contact angle and XPS, is improved using maleated rubbers.

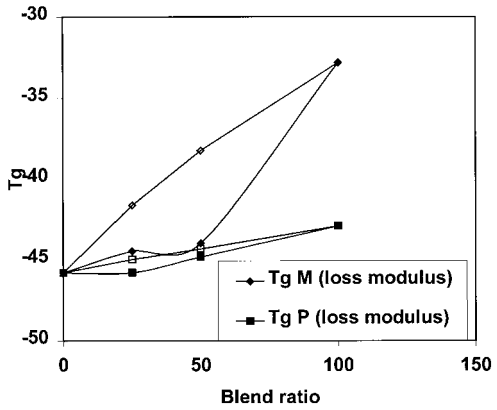

Figure 17 Effect of the gum rubber blends ratio on T_g.

- Peel strength results show that a higher maleic anhydride content in grafted rubber offers better adhesion with an EPDM compound.
- Rheological studies on first normal stress difference of grafted rubber and EPDM indicate the formation of droplets of maleated EPDM in EPDM.
- TEM studies of morphology further confirm the observation that, at a particular blend ratio (25%), the domain size is smaller with 1% than with 0.5% maleated rubber ($\sim$ 0.04 ca. 0.14 μm).
- All blends are heterogeneous, although the degree of dispersion is different.
- A single T_g is observed from DMA for P samples, whereas M samples show a broader transition. All blends show T_g's intermediate between two parent polymers. DMA also confirms the interaction between the components. As the strength of interaction increases, the T_g moves to a higher temperature with a concomitant decrease in tan δ height, in most cases.

The authors are thankful to Prof. James Mark and Prof. Wim van Ooij of the University of Cincinnati for organizing the TEM work, and to Dr. A. K. Bhattacharya of Rubber Technology Center IIT India and to Dr. John Wefer of Uniroyal Chemicals for supplying the maleated rubbers.

REFERENCES

1. Vanderaar, C. P. J.; Vanderdoes, L.; Noordermeer, J. W. M.; Bantjes, A.; Roseboom, F. Kautschuk Gummi Kunsts 1998, 51, 176.
2. Mirzadeh, H.; Katbab, A. A.; Burford, R. P. Radiat Phys Chem 1995, 46, 859.
3. Haddadiasi, V.; Burford, R. P. Radiat Phys Chem 1996, 47, 907.
4. Frederich, J. F.; Under, W.; Lippitz, A.; Gross, T.; Rohrer, P.; Saur, W.; Erdmann, J.; Gorsler, H. J Adhes Sci Technol 1995, 9, 575.
5. Roland, C. M. in Handbook of Elastomers: New Developments and Technology; Bhowmick, A. K.; Stephens, H. L., Eds.; Marcel Dekker: New York, 1988, p. 183.
6. Kole, S.; Santra, R.; Bhowmick, A. K. Rubber Chem Technol 1994, 67, 119.
7. Phan, T. T. M.; Denicola, A. J.; Schadler, L. S. J Appl Polym Sci 1998, 68, 1451.
8. Maity, K.; Xavier, S. F. Eur Polym J 1999, 35, 173.
9. Go, J. H.; Ha, C. S. J Appl Polym Sci 1996, 63, 509.
10. Coran, A. Y. Rubber Chem Technol 1988, 61, 281.
11. Yu, S. APRI J, 2000, June, 13.
12. Wu, S. Polymer Interface and Adhesion; Marcel Dekker: New York, 1982.
13. Choudhury, N. R.; Bhowmick, A. K. J Adhes Sci Technol 1988, 2, 167.
14. Hayes, R. A. Chem Aust 1992, October, 524.
15. Fowkes, F. M. Ind Eng Chem 1964, 56, 40.
16. Ginic-Markovic, M.; Choudhury, N. R.; Dimopoulos, M.; Dutta, N. K.; Matisons, J. G.; Bhattacharya, A. K. Polym Eng Sci 2000, 40, 1065.
17. Fox, T. G. Bull Am Phys Soc 1956, 1, 123.
18. Extrand, C. W.; Kumagai, Y. J Colloid Interface Sci 1997, 191, 378.
19. Garbassi, F.; Morra, M.; Occhiello, E. Polymer Surfaces from Physics and Technology; Wiley: Chichester, 1995/1996.
20. Owen, J. Ind Eng Chem Prod Res Dev 1980, 19, 97.
21. Busscher, H. J.; Van Pelt, A. W. J.; De Boer, P.; De Jong, H. P.; Arends, J. Colloids Surf 1984, 9, 319.
22. Holly, F.; Refojo, M. F. J Biomed Mater Res 1975, 9, 315.
23. Andrade, J. D., Ed. Surface and Interfacial Aspects of Biomedical Polymers, Vol. 1; Plenum Press: New York, 1985.
24. Mansfield, K. F.; Theodorou, D. N. Macromolecules 1991, 24, 6283.
25. Dimopoulos, M.; Choudhury, N. R.; Ginic-Markovic, M.; Matisons, J. G.; Williams, D. R. G. J Adhes Sci Technol 1998, 12, 1377.
26. Schultz, J.; Carre, A.; Mazeau, C. Int J Adhes 1984, 4, 163.
27. Lavielle, L.; Schultz, J. J Colloid Interface Sci 1985, 106, 438.
28. Jagur-Grodzinski, J. Heterogeneous Modification of Polymers; Wiley: Chichester, 1997.
29. Ghosh, M. K.; Das, C. K. J Appl Polym Sci 1994, 51, 643.
30. Kubota, H. J Appl Polym Sci 1975, 19, 2299.
31. Lee, B. L.; White, J. L. Trans Soc Rheol 1975, 19, 481.
32. Lin, C. Polym J 1979, 11, 185.
33. Utracki, L. A.; Fisa, B. Polym Compos 1982, 3, 193.
34. Corish, J. in Science and Technology of Rubber; Mark, J. E.; Erman, B.; Eirich, F. R., Eds.; Academic Press: New York, 1994; p. 545.
35. Avgeropoulos, G. N.; Weissert, F. C.; Biddison, P. H.; Bohm, G. G. A. Rubber Chem Technol 1976, 49, 93.
36. Wu, S. Polym Eng Sci 1987, 27, 335.
37. Kaplan, D. S. J Appl Polym Sci 1976, 20, 2615.
38. Roland, C. M. Macromolecules 1987, 20, 2557.
39. Nielsen, L. E. Mechanical Properties of Polymers; Reinhold Publishing/Chapman & Hall: London, 1962.
40. Plans, J.; MacKnight, W. J.; Karasz, F. E. Macromolecules 1984, 17, 810.
41. Utracki, L. A. Polymer Alloys and Blends; Hanser Publishers: New York, 1989.
42. Brazier, D. W.; Nickel, G. H. Thermochim Acta 1978, 26, 399.